EXPERIMENTAL ANALYSIS OF DIPOLE MODES IN ELLIPTICAL CAVITY*

M. Lalayan, A. Orlov, Ya. Shashkov, N. Sobenin,
National Research Nuclear University MEPhI, Moscow, Russia

Abstract

The experimental measurements of transverse shunt impedance for higher order modes TM_{110} and TE_{111} for S-band elliptical cavity were carried out. The experiments using dielectric and metallic spheres as perturbing objects and with ring probe were done.

INTRODUCTION

While studying the accelerating structures besides the calculation of electrodynamic characteristics (EDCs) at operating mode and higher order modes (HOMs) it is important to determine these parameters experimentally.

Today a considerable number of universally acknowledged numerical simulation codes used for EDCs calculation is known. Possibilities of an experimental study are modest compared to the ones of simulation approach and depend on the availability of modern measuring equipment and methods.

The most well-known field measurement method is the small perturbation technique using dielectric and/or metal perturbing bodies of different shapes. This article presents the results of measurements of the transverse shunt impedance using this method. In addition to the known approaches [1-2] application of ring-type perturbing bead is considered [3].

CAVITY MODEL

All simulations were done using software to model of elliptical harmonic cavity without drift tubes [4]. Figure 1 shows the cavity cell geometry together with basic dimensions and illustrates principle of cavity design.

We considered two dipole modes TM_{110} and TE_{111}, as they are the most dangerous for beam dynamics.

There are two methods of calculating linear transverse shunt impedance $r_{sh\perp}$ [5]:

1. By using Panofsky–Wenzel (PW) theorem one could derive the following equation:

$$r_{sh\perp} = \frac{\int_0^l \frac{1}{k_z}\frac{\partial E_z}{\partial r}\exp(ik_z z)dz}{P_{loss}*l} \quad (1)$$

where k_z - longitudinal wave number, E_z – longitudinal component of the electric field, P_{loss} – power loss in the structure, r – transverse coordinate offset in the plane of the dipole polarization of the wave off the cavity axis, l – length of the structure.

2. The direct integration (DI) method based on the transverse components of the electric $E_y(z)$ and magnetic $H_x(z)$ fields calculation.

$$r_{sh\perp} = \frac{\left|ic*\mu_0*\int_0^l H_z(z)\exp(ik_z z)dz - \int_0^l E_y(z)\exp(ik_z z)dz\right|}{P_{loss}*l} \quad (2)$$

where c – speed of light , μ_0 – magnetic constant.

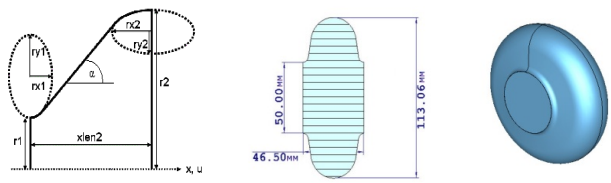

Figure 1: Geometry of elliptical harmonic cavity cell.

PERTURBING BODIES

Dielectric (DS), metallic (MS) spheres and metal wire loop probe as perturbing bodies were used for our research.

Table 1. Characteristics of Ceramic and Metallic Spheres

Parameter	simulation	experiment
Diameter, mm	1,8	1,8
DS form-factor k^E*10^{-20}, $(m^2\times s)/Ohm$	1,50	1,32
Electric constant	9,4	
MS form-factor k^E*10^{-20}, $(m^2\times s)/Ohm$	2,03	1,87
MS form-factor k^H*10^{-15}, $m^2\times s\times Ohm$	1,44	1,19

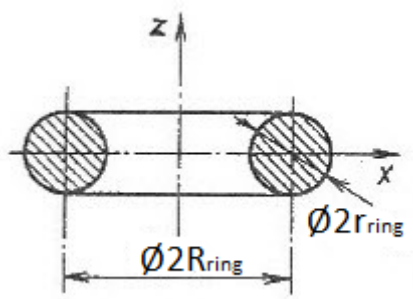

Figure 2: Geometry of ring probe.

Ring probe as bead for magnetic field and axially symmetric electric fields measurements is considered in [3]. Ring probe shape and dimensions are illustrated by

*Work supported by Ministry of Education and Science grant 3.245.2014/r

ISBN 978-3-95450-181-6

Figure 2. Electric and Magnetic form-factors for the ring probe can be calculated using the following formulas:

$$k_z^E = \varepsilon_0 \pi^2 r_{ring}^2 R_{ring} \quad (3)$$

$$k_z^M \cong \frac{\mu_0 \pi^2 R_{ring}^3}{4\ln(\frac{R_{ring}}{r_{ring}})} \quad (4)$$

The ring probe has larger orientation coefficient in a magnetic field compared to the metal sphere, i.e. ratio of the longitudinal form-factor to the transverse one.

$$k_{dir}^M = \frac{k_z^M}{k_{x,y}^M} = \frac{1}{3}\left(\frac{R_{ring}}{r_{ring}}\right)^2 \frac{1}{ln\left(\frac{R_{ring}}{r_{ring}}\right)} \quad (5)$$

Table 2. Characteristics of Metallic Ring Probe

Parameter	Simulation	Experiment
R_{ring}, mm	2,30	2,30
r_{ring}, mm	0,35	0,35
form-factor k^E*10^{-19}, (m^2×s)/Ohm	2.01	2.38
form-factor k^H*10^{-14}, m^2×s×Ohm	2,00	1,92

As it could be seen from Tables 1 and 2, the ring form-factor for the magnetic field is considerably greater than one for metallic sphere.

EXPERIMENTAL RESULTS

Ceramic and metallic spheres with the characteristics presented in Table 1 and ring probe as perturbing bodies were chosen and used for measurements. The experimental stand is described in [5].

During the pulling of perturbing body in the cavity phase change of transmission coefficient S_{21} with respect to phase, with the perturbing body is out of the cavity was measured. The corresponding change in the resonance frequency _ is calculated from the following formula (where Q_L – loaded Q-factor)

$$\frac{\Delta f}{f_0} = \frac{1}{2 * Q_L}\tan(\Delta\varphi) \quad (6)$$

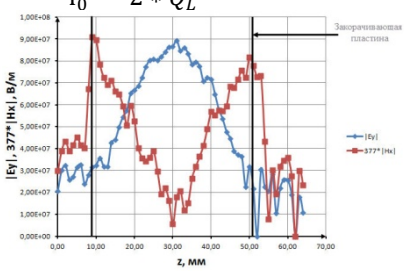

Figure 3: Distribution of fields.

Figure 3 shows the distribution of the transverse components of the electric and magnetic fields. Change in the resonance frequency was measured with ceramic and metallic spheres moved along the longitudinal cavity axis.

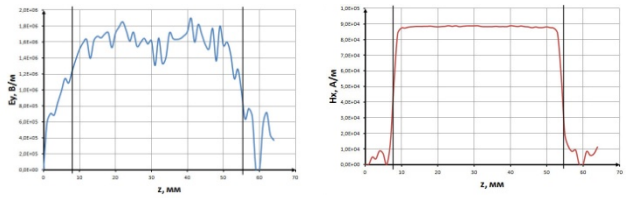

Figure 4: Distribution of transverse component of fields for TM_{110}.

Figure 4 shows the transverse field components distribution. Simulation of the experiment was carried out with ceramic and metallic spheres resulting in the same dependencies.

Figures 5 and 6 show results of experimental fields measurements using te metallic ring and ceramic sphere.

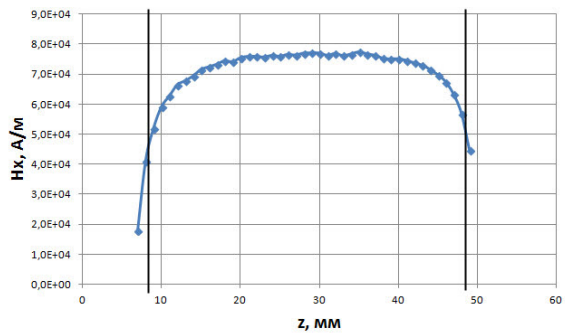

Figure 5: Distribution of magnetic field $|H_x|$ in measurements for TM_{110}.

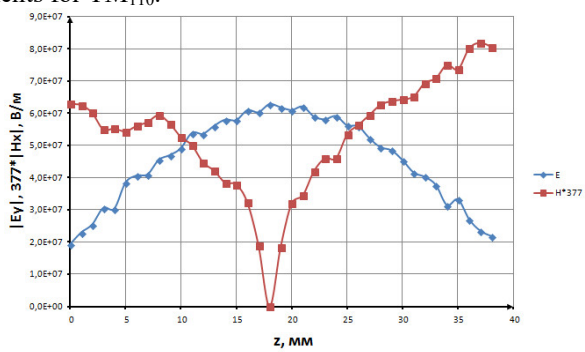

Figure 6: Distribution of fields in measurements for TE_{111}.

ERROR ESTIMATIONS

In the experiments the following uncertainty sources were considered: instrumental error, error in measurement of resonant frequency change, phase change of transmission factor, the loaded Q – factor, as well as manufacturing tolerances of perturbing bodies, perturbing body guide and positioning system.

Figures 7-8 show change form-factor of perturbing bodies when their size changes.

ISBN 978-3-95450-181-6

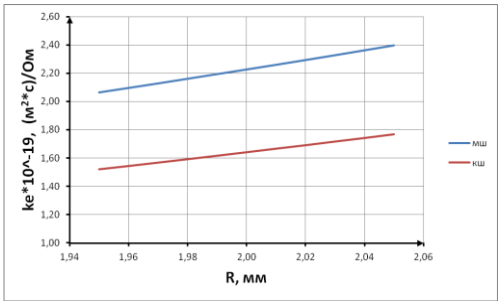

Figure 7: The dependence of the electric form-factor for spheres vs radius.

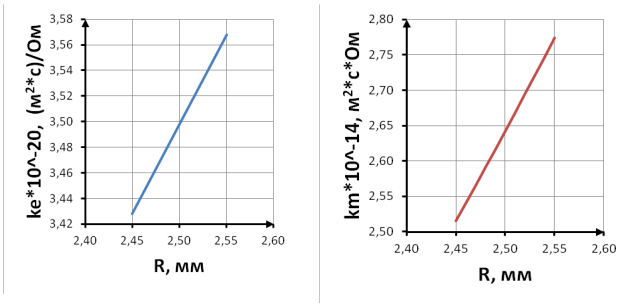

Figure 8: The dependence of form-factors for ring probe vs. radius at constant cross-section radius r = 0,4 mm.

Accuracy of the measurement fields using the ring probe was estimated in case of the ring is tilted by a small angle (10-20°) about to the magnetic field lines. The evaluation was done for TM_{110} mode. Figure 9 shows that in the case of 10 degrees deviation resulting field strength error is 1,5%, and in the case of 20 degrees it is 6%.

The total error in measurements is 11-18%.

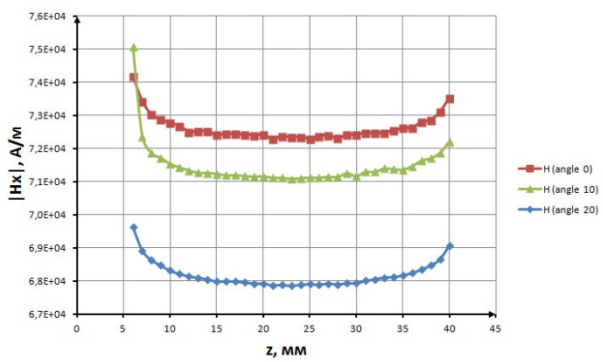

Figure 9: Transverse component of the magnetic field $|H_x|$ distribution along the structure.

TRANSVERSE SHUNT IMPEDANCE

After that based on the field measurement results the shunt impedance values were obtained and compared to the results obtained by the simulation results. The $r_{sh\perp}$ values were calculated by the the formulas (1) and (2). The comparison of the results obtained with different measurement methodics are presented in Table 3.

Table 3. Comparison of results obtained by different measurement methodics.

Wave		$r_{sh\perp}$, MOhm/m	
		TM_{110}	TE_{111}
Computer simulation	PW	17	0,76
	DI	16	0,76
Simulation of experiment	PW	14,0	
	DI (sphere)	16,0	0,89
	DI (ring)	17	0,84
Experiment	PW	13,7	
	DI (sphere)	16,9	0,77
	DI (ring)	16,5	0,86

CONCLUSION

The measurements of transverse shunt impedance for dipole modes TM_{110} and TE_{111} using ceramic, metallic spheres and ring probe were performed. The results showed the measurements done by the ring probe have the accuracy not worse than with the use of spherical probe.

REFERENCE

[1] M. Navarro-Tapia, R. Calaga, Bead-Pull measurements of the main deflecting mode of the double-quarter-wave cavity for the HL-LHC, proceedings of SRF2015, Pre-Press, Whistler, BC, Canada.

[2] H. Hahn, R. Calaga, HOM identification by bead pulling in the Brookhaven ERL cavity, Nuclear Instruments and Methods in Physics Research A 734 (2014) 72–78.

[3] B.V. Zverev, N.P. Sobenin, Electrodynamic Characteristics of Accelerating Cavities, Energoatomizdat, Moscow, 1993.

[4] Ya. V. Shashkov et al. “Comparison of higher order modes damping techniques for 800 MHz single cell superconducting cavities”, Nuclear Instruments and Methods in Physics Research A, v. 767, 2014.

[5] A.A. Zavadtsev, D.A. Zavadtsev, V.I. Kaminsky, A.Yu. Smirnov, N.P. Sobenin, “RF deflectors for the diagnostic of charged particles beams”, M:NRNU MEPhI, 2014, 180 p. (in Russian).

ISBN 978-3-95450-181-6